ACS OMEGA

Article

Cite This: ACS Omega 2017, 2, 7682-7685

http://pubs.acs.org/journal/acsodf

Enhanced Transverse Magneto-Optical Kerr Effect in Magnetoplasmonic Crystals for the Design of Highly Sensitive Plasmonic (Bio)sensing Platforms

B. F. Diaz-Valencia,[†,∥] J. R. Mejía-Salazar,[‡] Osvaldo N. Oliveira, Jr.,[‡] N. Porras-Montenegro,[†] and Pablo Albella*[,§,⊥]

[†]Department of Physics, University of Valle, A.A 25360 Cali, Colombia

[‡]Instituto de Física de São Carlos, University of São Paulo, CP 369, 13560-970 São Carlos, SP, Brasil

[§]University Institute for Intelligent Systems and Numerical Applications in Engineering (SIANI), University of Las Palmas de Gran Canaria, 35017 Las Palmas de Gran Canaria, Spain

[∥]Centre for Bioinformatics and Photonics-CIBioFi, Calle 13 No. 100-00, Edificio 320 No. 1069, A.A 25360 Cali, Colombia

[⊥]The Blackett Laboratory, Department of Physics, Imperial College London, London SW7 2AZ, U.K.

ABSTRACT: We propose a highly sensitive sensor based on enhancing the transversal magneto-optical Kerr effect (TMOKE) through excitation of surface plasmon resonances in a novel and simple architecture, which consists of a metal grating on a metal magneto-optical layer. Detection of the change in the refractive index of the analyte medium is made by monitoring the angular shift of the Fano-like resonances associated with TMOKE. A higher resolution is obtained with this technique than with reflectance curves. The key aspect of the novel architecture is to achieve excitation of surface plasmon resonances mainly localized at the sensing layer, where interaction with the analyte occurs. This led to a high sensitivity, $S = 190°\ \mathrm{RIU}^{-1}$, and high performance with a figure of merit of the order of 10^3, which can be exploited in sensors and biosensors.

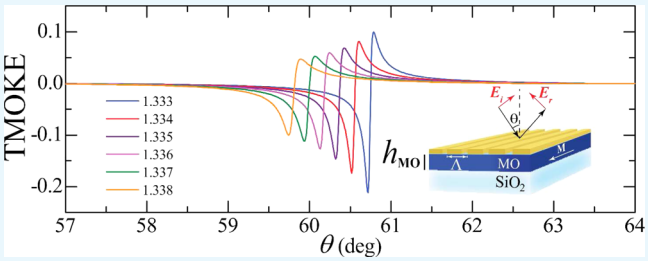

INTRODUCTION

Surface plasmon resonances (SPRs) are charge density oscillations on metal/dielectric interfaces, which allow for concentrating electromagnetic energy to be employed in applications at nanoscale dimensions.[1−4] This electromagnetic field localization is sensitive to the dielectric properties of the surrounding media, thus being suitable for plasmonic biosensors in addition to real-time monitoring of adsorption processes and studying the molecular interactions involved.[5−10] Because detection requires measurable changes in the refractive index of the analyte, this technique is mostly limited to detecting high-molecular-weight (large) biomolecules. Several efforts are being pursued to circumvent this limitation and improve the sensitivity of SPR-based sensing, including the combination of SPR spectroscopy and enzymatic detection,[11] use of hyperbolic materials[12] to develop ultrasensitive SPR biosensing platforms, and the use of magnetoplasmonic effects instead of SPRs for the detection of very small refractive index changes.[13−18] The idea behind the latter approach is to exploit the sharp Fano-like resonant plasmonic enhanced magneto-optical (MO) effects instead of broad plasmonic resonances. This concept has been explored in magnetoplasmonic superlattices in the Kretschmann configuration[14,15] and magnetoplasmonic crystals.[16−18] Magnetoplasmonic crystals made as one- or two-dimensional arrays of metallic scatterers combined with magnetic layers are advantageous for miniaturization and integration with microfluidic systems, unlike the Kretschmann-like systems, where miniaturization is impaired by the need to use a prism with refractive index larger than the refractive index of the dielectric background. Enhanced TMOKE effects can be obtained with magnetoplasmonic crystals,[19−23] but improved SPR sensing/biosensing was only experimentally demonstrated during the last few years for one-dimensional grating structures.[17,18] High-performance magnetoplasmonic-based sensing platforms were proposed in a theoretical paper, which would be made of a two-dimensional grating structure with an array of metallic nanoholes in a trilayer of Au/Co/Au.[16] The proposed system is suitable for miniaturization and may be combined with microfluidic systems to implement real-time analysis of molecular binding events, but the precise construction of the nanoholes in Au/Co/Au trilayers may be difficult and expensive.[16]

In this work, we propose the design of a simple yet highly sensitive sensing platform made as a one-dimensional magnetoplasmonic crystal, consisting of a metal grating grown on a magneto-optical metallic substrate. Because the sensitivity of an SPR-based sensor (or biosensor) depends on where the

Received: September 29, 2017
Accepted: October 25, 2017
Published: November 8, 2017

DOI: 10.1021/acsomega.7b01458
ACS Omega 2017, 2, 7682−7685

electromagnetic field is most amplified, the idea is to develop a magnetoplasmonic crystal to excite SPRs mainly localized at the analyte region. This can be reached by optimizing the geometry of the grating structure and the MO metallic slab according to the incident wavelength.[23] By using the optimization procedure in ref 16, we show enhanced TMOKE values with very narrow Fano-like resonant peaks, which can be interrogated by monitoring either the angle or the wavelength. These Fano-like resonances are extremely sensitive to the refractive index of the surrounding media, thus allowing to detect very small changes in the dielectric properties of the analyte.

RESULTS AND DISCUSSION

The magnetoplasmonic system proposed here, to be grown on a SiO_2 substrate, is shown in Figure 1. It consists of Au metal

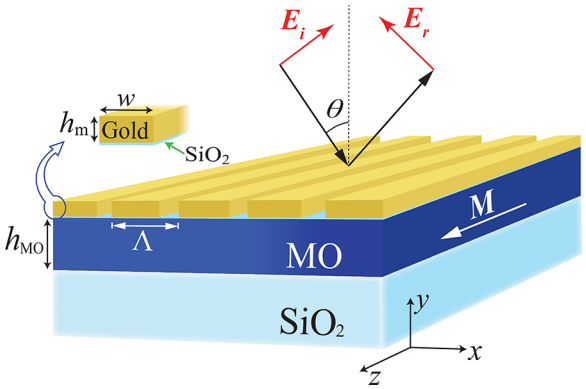

Figure 1. Schematic diagram of the proposed sensor platform, where h_m and h_{MO} are the thicknesses of the metallic and MO materials, respectively, and w is the width of the metal grating. Λ is the grating period. The magnetization vector, **M**, is parallel to the z axis.

gratings on top of a planar metallic MO layer with a 2 nm thick layer of SiO_2 in between. The magnetization (**M**), or external applied magnetic field, is considered along the z axis; thus, the dielectric permittivity tensor is written as

$$\breve{\varepsilon} = \begin{pmatrix} \varepsilon_0 & ig & 0 \\ -ig & \varepsilon_0 & 0 \\ 0 & 0 & \varepsilon_0 \end{pmatrix} \quad (1)$$

where ε_0 is the dielectric function of the non-magnetized film (i.e., without magnetic field/magnetization) and g takes into account the MO activity. These values are considered as $\varepsilon_0 = -10.51 + 2.1i$ and $g = -1.2 + 1.15i$, corresponding to Co_6Ag_{94} material under a working wavelength of $\lambda = 631$ nm,[24] measured at room temperature after annealing at 250 °C.

To excite an SPR, the wavevector of the incoming light needs to be matched to the one for a surface plasmon, $k_{SPR} = k_0\sqrt{\frac{\varepsilon_m n_{an}^2}{\varepsilon_m + n_{an}^2}}$, propagating at a metal/dielectric interface. This can be done through the diffraction mechanism by using the diffraction grating in Figure 1, where the incident beam is split into a series of beams with the wavevector along the interface altered as $k_x + q\frac{2\pi}{\Lambda} = k'_{x\Lambda}$. Then, the condition for SPR excitation is given by

$$\pm k_0\sqrt{\frac{\varepsilon_m n_{an}^2}{\varepsilon_m + n_{an}^2}} = k_0 n_{an}\sin(\theta) + \frac{2\pi}{\Lambda}q \quad (2)$$

where Λ is the period of the grating, n_{an} is the analyte refractive index, ε_m is the permittivity of the metal, $k_0 = \frac{\omega}{c}$, and q is the diffraction order. The signs $\pm$ are for $q > 0$ and $q < 0$, respectively. θ is the resonance angle at which the plasmonic resonance occurs. The grating period and the width of the gold gratings were chosen as $\Lambda = 250$ nm and $w = 225$ nm, respectively, thus having a negative diffractive order $q = -1$.[25]

Because the main interest is to exploit the magnetoplasmonic effect in the transversal configuration, we make use of the well-known TMOKE parameter, which can be defined as

$$\text{TMOKE} = \frac{R_{pp}(+\mathbf{M}) - R_{pp}(-\mathbf{M})}{R_{pp}(+\mathbf{M}) + R_{pp}(-\mathbf{M})} \quad (3)$$

and measures the relative change in reflectance for p-polarized (TM-polarized) incident light, R_{pp}, when the magnetization (applied magnetic field) of the MO layer is reversed. Signs $\pm$ for **M** refer to the magnetization pointing along the (0, 0, $\pm$ 1) directions. All numerical results we show in this work were obtained using the finite element method (COMSOL Multiphysics).

For developing an optimized one-dimensional grating structure for SPR-based sensing/biosensing, we first need to optimize the geometry of the metallic gratings to have very sharp TMOKE resonances with enhanced amplitudes. Figure 2 shows

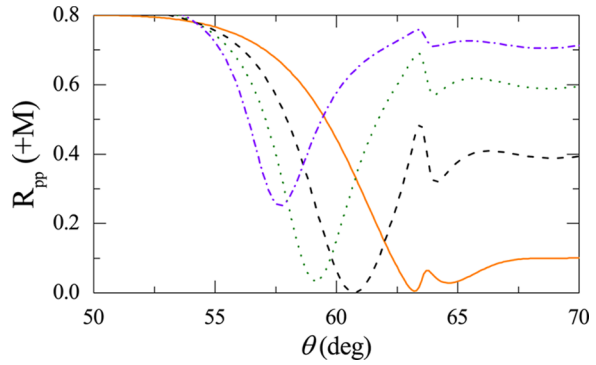

Figure 2. Reflectance as a function of θ for various thicknesses h_m, using $\Lambda = 250$ nm and $h_{MO} = 80$ nm. The solid, dashed, dotted, and dash-dotted curves are for $h_m = 50$, 70, 90, and 110 nm, respectively.

the reflectance as a function of θ for various thicknesses of the Au grating, h_m, with the analyte refractive index being $n_{an} = 1.333$ to be compatible with an aqueous environment for the analyte, and the MO layer thickness is $h_{MO} = 80$ nm. The minima in the reflectance curves associated with plasmonic resonances change with the thickness of the different Au gratings. From these curves, the deeper reflectance curve occurs for $h_m = 70$ nm, thus indicating an optimized coupling of the incident light to SPRs in the structure for the working wavelength. Therefore, henceforth we use $h_m = 70$ for the Au grating.

After this optimization of the light−matter coupling, we search for the optimal MO layer thickness that leads to the highest TMOKE values. Figure 3a shows TMOKE as a function of θ for different MO layer thicknesses, h_{MO}, from where it can be noted that TMOKE resonance becomes sharp around the same θ value as h_{MO} increases. Also, above $h_{MO} = 120$ nm, there is no further

DOI: 10.1021/acsomega.7b01458
ACS Omega 2017, 2, 7682−7685

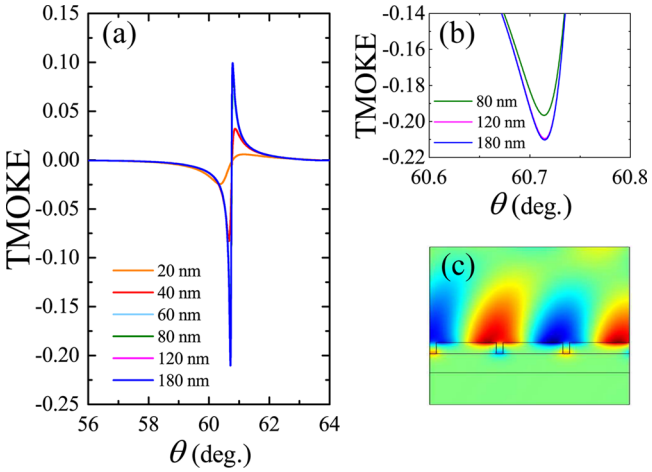

Figure 3. (a) TMOKE as function of the incident angle, θ, for different values of h_{MO}. (b) Comparison of TMOKE for three values of h_{MO} in a zoomed figure to show that no changes occur for h_{MO} above 120 nm. (c) Magnitude of magnetic field $|H_z|$, in which the excitation of SPRs at the analyte−metallic interface is highlighted. Calculations were made by considering h_m = 70 nm.

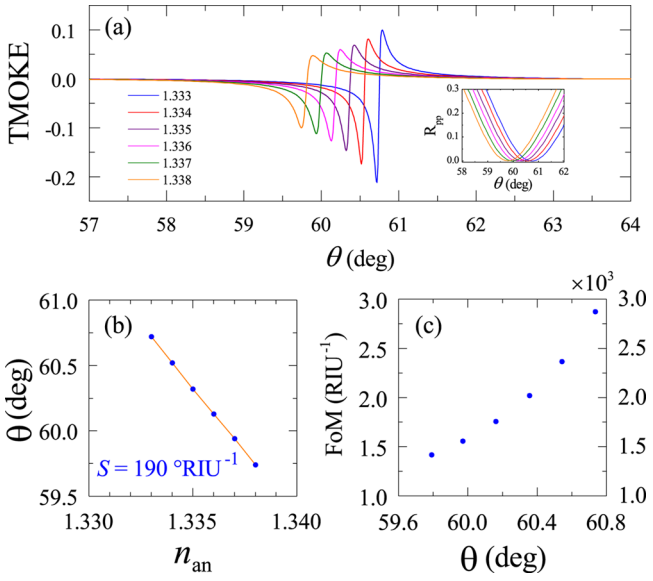

Figure 4. (a) TMOKE as a function of the incidence angle, θ, for different values of n_{an}. The inset shows the reflectance curves, R_{pp}(+**M**), around the SPP resonances. (b) Solid circles show the minima of TMOKE curves in (a) as a function of n_{an}, whereas the solid line corresponds to a linear fitting with a slope of −190° RIU^{-1}, thus producing a sensitivity of S = 190° RIU^{-1}. (c) Figure of merit for the optimized system, as a function of the resonant angle (see eq 4 for the definition).

increase in TMOKE, as shown in Figure 3b. Therefore, we fix h_{MO} = 120 nm to have optimal TMOKE amplitudes. With this optimized geometry, the field profile of $|H_z|$ for the resonant angle θ = 60.7° shows strong localization in the analyte medium according to Figure 3c. This will enhance the dependence of the SPP resonance on the dielectric properties of this medium. The sensing performance is quantified by following the usual practice of defining the bulk refractive index sensitivity as $S = \left|\frac{\Delta\theta}{\Delta n_i}\right|$, where $\Delta\theta$ is the shift of the Fano-like resonance and Δn_i is the change in refractive index of the incident medium. Because gold gratings can be easily functionalized for sensing purposes, in Figure 4a we show as a practical example the proposed magnetoplasmonic platform as a sensing/biosensing system. Significantly, this platform is able to detect very small changes in the refractive index in the analyte medium, with a sensitivity S = 190° RIU^{-1}, as seen in the results in Figure 4b, which is similar to that of more complex proposals.[16] As pointed out in ref 16, the performance of this magnetoplasmonic-based sensing platform is characterized by the ratio FoM = S/Γ, where S and Γ are the sensitivity and line width of the Fano-like feature, respectively. Γ is obtained by fitting the TMOKE curves as a function of θ to a Fano line shape of the form[16,26]

$$\text{TMOKE} = A + B\frac{(r\Gamma/2 + \theta - \theta_0)^2}{(\Gamma/2)^2 + (\theta - \theta_0)^2} \quad (4)$$

where θ_0 is the resonant angle, r is the Fano parameter, and A and B are fitting values. This analysis leads us to a figure of merit (FoM) with values in the same order as the ones presented in ref 16.

CONCLUSIONS

In conclusion, we have demonstrated that one-dimensional magnetoplasmonic structures can be easily optimized to produce highly sensitive sensing/biosensing applications with similar performance to more sophisticated structures. The proposed platform is made by just a gold grating on a magneto-optical material, being therefore experimentally feasible. The sensitivity predicted of S = 190° RIU^{-1} is high and promising for state-of-the-art sensors and biosensors.

AUTHOR INFORMATION

Corresponding Author

*E-mail: pablo.albella@ulpgc.es.

ORCID

J. R. Mejía-Salazar: 0000-0003-1742-9957

Pablo Albella: 0000-0001-7531-7828

Notes

The authors declare no competing financial interest.

ACKNOWLEDGMENTS

The authors acknowledge the financial support from the Brazilian Agencies CNPq and FAPESP (2013/14262-7 and 2016/12311-9). B.F.D.-V. acknowledges support from CIBioFi, the Colombian Science, Technology and Innovation Fund - General Royalties System (Fondo CTeI-SGR), Gobernación del Valle del Cauca, and COLCIENCIAS, under contract No. BPIN 2013000100007. P.A. acknowledges Programa "Viera y Clavijo" de la Agencia Canaria de Investigación, Innovación y Sociedad de la Información (ACIISI) y la Universidad de las Palmas de Gran Canaria (ULPGC).

REFERENCES

(1) Wurtz, G. A.; Pollard, R.; Zayats, A. V. Optical bistability in nonlinear surface-plasmon polaritonic crystals. *Phys. Rev. Lett.* **2006**, *97*, No. 057402.

(2) Hoa, X. D.; Kirk, A. G.; Tabrizian, M. Towards integrated and sensitive surface plasmon resonance biosensors: a review of recent progress. *Biosens. Bioelectron.* **2007**, *23*, 151−160.

(3) Kneipp, K. Surface-enhanced Raman scattering. *Phys. Today* **2007**, *11*, 40.

DOI: 10.1021/acsomega.7b01458
ACS Omega 2017, 2, 7682−7685

(4) Zhou, W.; Dridi, M.; Suh, J. Y.; Kim, C. H.; Co, D. T.; Wasielewski, M. R.; Schatz, G. C.; Odom, T. W. Lasing action in strongly coupled plasmonic nanocavity arrays. *Nat. Nanotechnol.* **2013**, *8*, 506−511.
(5) Deckert, F.; Legay, F. Development and validation of an immunoreceptor assay for simulect based on surface plasmon resonance. *Anal. Biochem.* **1999**, *274*, 81−89.
(6) Iwasaki, Y.; Horiuchi, T.; Niwa, O. Detection of Electrochemical Enzymatic Reactions by Surface Plasmon Resonance Measurement. *Anal. Chem.* **2001**, *73*, 1595−1598.
(7) Karlsson, R. SPR for Molecular Interaction Analysis: A Review of Emerging Application Areas. *J. Mol. Recognit.* **2004**, *17*, 151−161.
(8) Vutukuru, S.; Bethi, S. R.; Kane, R. S. Protein Interactions with Self-Assembled Monolayers Presenting Multimodal Ligands: A Surface Plasmon Resonance Study. *Langmuir* **2006**, *22*, 10152−10156.
(9) Shankaran, D. R.; Gobi, K. V.; Miura, N. Recent Advancements in Surface Plasmon Resonance Immunosensors for Detection of Small Molecules of Biomedical, Food and Environmental Interest. *Sens. Actuators, B* **2007**, *121*, 158−177.
(10) Wang, J.; Wang, F.; Chen, H.; Liu, X.; Dong, S. Electrochemical surface plasmon resonance detection of enzymatic reaction in bilayer lipid membranes. *Talanta* **2008**, *75*, 666−670.
(11) Miyazaki, C. M.; Shimizu, F. M.; Mejía-Salazar, J. R.; Oliveira, O. N., Jr.; Ferreira, M. Surface Plasmon Resonance Biosensor for Enzymatic Detection of Small Analytes. *Nanotechnology* **2017**, *28*, No. 145501.
(12) Sreekanth, K. V.; Alapan, Y.; ElKabbash, M.; Ilker, E.; Hinczewski, M.; Gurkan, U. A.; De Luca, A.; Strangi, G. Extreme sensitivity biosensing platform based on hyperbolic metamaterials. *Nat. Mater.* **2016**, *15*, 621.
(13) Regatos, D.; Sepúlveda, B.; Fariña, D.; Carrascosa, L. G.; Lechuga, L. M. Suitable combination of noble/ferromagnetic metal multilayers for enhanced magneto-plasmonic biosensing. *Opt. Express* **2011**, *19*, 8336−8346.
(14) Manera, M. G.; Ferreiro-Vila, E.; García-Martin, J. M.; García-Martin, A.; Rella, R. Enhanced antibody recognition with a magneto-optic surface plasmon resonance (MO-SPR) sensor. *Biosens. Bioelectron.* **2014**, *58*, 114−120.
(15) Ignatyeva, D. O.; Knyazev, G. A.; Kapralov, P. O.; Dietler, G.; Sekatskii, S. K.; Belotelov, V. I. Magneto-optical plasmonic heterostructure with ultranarrow resonance for sensing applications. *Sci. Rep.* **2016**, *6*, No. 28077.
(16) Caballero, B.; Garcia-Martín, A.; Cuevas, J. C. Hybrid magnetoplasmonic crystals boost the performance of nanohole arrays as plasmonic sensors. *ACS Photonics* **2016**, *3*, 203−208.
(17) Chou, K.-H.; Lin, E.-P.; Chen, T.-C.; Lai, C.-H.; Wang, L.-W.; Chang, K.-W.; Lee, G.-B.; Lee, M.-C. M. Application of strong transverse magneto-optical Kerr effect on high sensitive surface plasmon grating sensors. *Opt. Express* **2014**, *22*, 19794.
(18) Grunin, A. A.; Mukha, I. R.; Chetvertukin, A. V.; Fedyanin, A. A. Refractive index sensor based on magnetoplasmonic crystals. *J. Magn. Magn. Mater.* **2016**, *415*, 72−76.
(19) Belotelov, V. I.; Bykov, D. A.; Doskolovich, L. L.; Kalish, A. N.; Zvezdin, A. K. Extraordinary transmission and giant magneto- optical transverse Kerr effect in plasmonic nanostructured films. *J. Opt. Soc. Am. B* **2009**, *26*, 1594.
(20) Grunin, A. A.; Zhdanov, A. G.; Ezhov, A. A.; Ganshina, E. A.; Fedyanin, A. A. Surface-plasmon-induced enhancement of magneto-optical Kerr effect in all-nickel subwavelength nanogratings. *Appl. Phys. Lett.* **2010**, *97*, No. 261908.
(21) Belotelov, V. I.; Bykov, D. A.; Doskolovich, L. L.; Kalish, A. N.; Zvezdin, A. K. Giant Transversal Kerr Effect in Magneto-Plasmonic Heterostructures: The Scattering-Matrix Method. *J. Exp. Theor. Phys.* **2010**, *110*, 816.
(22) Belotelov, V. I.; Akimov, I. A.; Pohl, M.; Kotov, V. A.; Kasture, S.; Vengurlekar, A. S.; Gopal, A. V.; Yakovlev, D. R.; Zvezdin, A. K.; Bayer, M. Enhanced magneto-optical effects in magnetoplasmonic crystals. *Nat. Nanotechnol.* **2011**, *6*, 370.
(23) Halagačka, L.; Vanwolleghem, M.; Postava, K.; Dagens, B.; Pištora, J. Coupled mode enhanced giant magnetoplasmonics transverse Kerr effect. *Opt. Express* **2013**, *21*, 21741.
(24) Wang, S.-Y.; Zheng, W.-M.; Qian, D.-L.; Zhang, R.-J.; Zheng, Y.-X.; Zhou, S.-M.; Yang, Y.-M.; Li, B.-Y.; Chen, L.-Y. Study of the Kerr effect of Co_xAg_{100-x} granular films. *J. Appl. Phys.* **1999**, *85*, 5121.
(25) Lin, K.; Lu, Y.; Chen, J.; Zheng, R.; Wang, P.; Ming, H. Surface plasmon resonance hydrogen sensor based on metallic grating with high sensitivity. *Opt. Express* **2008**, *16*, 18599.
(26) Yanik, A. A.; Cetin, A. E.; Huang, M.; Artar, A.; Mousavi, S. H.; Khanikaev, A.; Connor, J. H.; Shvets, G.; Altug, H. Seeing protein monolayers with naked eye through plasmonic Fano resonances. *Proc. Natl. Acad. Sci. U.S.A.* **2011**, *108*, 11784−11789.

DOI: 10.1021/acsomega.7b01458
ACS Omega 2017, 2, 7682−7685